

## Transport properties of in-plane MoS<sub>2</sub> heterostructures from lateral and vertical directions

Mei Ge, Xiaoyan Guo, and Junfeng Zhang\*

*School of Physics and Information Engineering, Shanxi Normal University, Linfen 041004, China.*

Received 11 September 2015; Accepted 21 October 2015

Published Online 1 March 2016

---

**Abstract.** Two-dimensional (2D) molybdenum disulfide (MoS<sub>2</sub>) promised a wide range of potential applications. Here, we report the transport investigations on the MoS<sub>2</sub> from Armchair (AC) and Zigzag (ZZ) directions with different kinds of leads. The conductance of 2H phase MoS<sub>2</sub> depended on the transport directions and lead types (2H phase or 1T phase). System with 1T phase MoS<sub>2</sub> as lead can impressively improve the transport properties compared with the 2H phase lead. Moreover, for the system with metal lead, enhanced conductance can be observed, which contrast to the experiment measurements. Further investigate indicated that the conductance is sensitively rely on the distance between metal lead and 2D material. The present theoretical results suggested the lead material and interface details are both important for MoS<sub>2</sub> transport exploration, which can provide vital insights into the other 2D hybrid materials.

**PACS:** 7340-c

**Key words:** lateral heterostructures, phase hybrid materials, MoS<sub>2</sub>, transport.

---

## 1 Introduction

Recently, two dimensional (2D) materials like molybdenum disulphide (MoS<sub>2</sub>) have attracted many interests because of them excellent physical and chemical properties and then promised many potential applications [1–8]. Monolayer MoS<sub>2</sub> appears in many distinct phases depending on the arrangement of its S atoms, two of them are more popular and exhibits substantially different electronic structures: 2H (trigonal prismatic,  $D_3h$ ) MoS<sub>2</sub> is a semiconductor with a finite band gap between the filled  $d_{z^2}$  and empty  $d_{x^2-y^2,xy}$  bands, and 1T (octahedral geometry,  $O_h$ ) phase is metallic with Fermi level lying in the middle of degenerate  $d_{xy,yz,xz}$  single band [9]. The reversible transition between

---

\*Corresponding author. *Email addresses:* zhangjf@sxnu.edu.cn (J.-F. Zhang)

2H and 1T phase have been proved by annealing [10], electric doping [11, 12], applying strain [13] or electron-beam irradiating [14]. Moreover, a mixed phase (2H and 1T) structure with the abrupt phase interface and matched lattice has been demonstrated experimentally [15]. This kind of bi-phase material paved a new way to design 2D photoelectric devices based on the in-plane metal/semiconductor heterostructures [16, 17].

Compared with the comprehensive studies on the fabrications [18–21] and applications [22, 23] of graphene/h-BN heterostructures, fewer reports focused on the in-plane 1T/2H MoS<sub>2</sub> hybrid systems. [14–16] By using lithium based chemical exfoliation method, Eda *et al.* [15] firstly synthesized a single layer of exfoliated MoS<sub>2</sub> consisting of both 2H and 1T phases then form chemically homogeneous atomic and electronic heterostructures with potential for novel molecular functionalities. The atomic phase transition mechanism for 2H to 1T in mono-layer MoS<sub>2</sub> have been explored with transmission electron microscopy, in which the controllable area of 1T phase was achieved with essential intermediate phases as the precursor phase [14].

Former studies suggested that the grain boundaries of the 2H monolayer MoS<sub>2</sub> have important effects on the transport properties [24]. They found that only tilt GBs have a significant effect on the mobility and transport characteristics of MoS<sub>2</sub>, and these kinds of effects rely mostly on the defect type and density. In another experimental measurement, by using the 1T phase MoS<sub>2</sub> electrodes and well controlled phase interface, the contact resistance of 2H MoS<sub>2</sub> can be significant reduced without the performance loss [16, 17]. They attribute the superior performance of the devices to absence of structural and electrical mismatch between 1T and 2H MoS<sub>2</sub>.

In this paper, we performed a first-principle combine with non-equivalent transport investigations on the 2H monolayer MoS<sub>2</sub> hybrid system with 1T and 2H electrodes. We focused on the relationship between the thermodynamics stability of the 1T/2H interface, and transport properties with different kinds of the electrodes. We found that the intermediate phase is unavoidable, and system's conductance is affected by electrodes choices.

## 2 Theoretical methods

The atomic and electronic structures of the 1T/2H monolayer MoS<sub>2</sub> phase interfaces were investigated using the DFT and the projector-augmented wave method (PAW) [25], as implemented in the Vienna ab-initio simulation package (VASP) [26]. The exchange-correction interaction was described by the Perdew-Burke-Ernzerhof (PBE) [27] functional. The plane-wave basis was expanded up to 550 eV. The 2D Brillouin zones of different interfaces were sampled by a series of k-point grids with constant separations of 0.02 Å<sup>-1</sup> during geometry optimization and 0.01 Å<sup>-1</sup> in the DOS calculation. 2D periodic boundary condition was applied in the directions along (y) and perpendicular (x) to the 1-dimensional (1D) interface. A single layer of molybdenum disulfide consists of a 6.7 Å thick slab of a S-Mo-S sandwich layer, [28] here a thickness of 20 angstrom was selected

in the (z) direction perpendicular to the MoS<sub>2</sub> sheet to avoid the interaction between periodic images. The atomic coordinates in xyz dimensions were fully relaxed without any constraint to allow possible out-of-plane inflection.

The transport properties of 2H MoS<sub>2</sub> were investigated combines first-principle technique with the Keldysh nonequilibrium Green's function. Real space linear combination of atomic orbital (LCAO) basis set of DZP was employed. The quantum conductance and quantum transmission were calculated by including self-energies for the coupling of a maximum 5-nm-wide scattering region to the semi-infinite 1T and 2H with/without metal leads under the zero-bias voltage.

### 3 Results and discussion

#### A. Structural and thermodynamically stability.

Within the GGA-PBE level, the calculated band gap of 2H MoS<sub>2</sub> is 1.66 eV (semiconducting) and more stable than metallic 1T MoS<sub>2</sub> with total energy 0.283 eV per atoms, which are consistent with the previous report [12]. By gliding only one plane S atoms in MoS<sub>2</sub> to the center of the hexagonal, semiconducting 2H phase will gradually transit to metallic 1T phase. Our theoretical investigations also suggested a transition energy barrier (1.04 eV) from the metastable 1T phase MoS<sub>2</sub> to the corresponding stable 2H phase. We have constructed the lateral 1T/2H heterostructures with an half of 2H domains and an half of 1T domains (as shown in Fig. 1) with AC and ZZ interfaces. As shown in Fig. 1a (AC type interface) and Fig.1b (ZZ type interface), the hybrid system have no atom loss or affluence in a supercell with atomically sharp interface as observed experimentally [15]. The supercell of the hybrid system have fixed periodic length along the interface (y direction) and different lengths (from 0.638 nm to 6.362 nm for AC and from 1.105 nm to 7.738 nm for ZZ interface, respectively) perpendicular to the interface (x direction). With the full atomic relaxations, the hexagonal arrangement of Mo and its orientation remains less disturbed across the boundary. The formation energies of the phase interfaces can be determined by:

$$E_{form} = (E_{hybrid} - N_{Mo} \times E_{Mo} - N_{S-2H} \times E_{S-2H} - N_{S-1T} \times E_{S-1T}) / d, \quad (1)$$

here,  $E_{hybrid}$  is the total energy of the hybrid system,  $N_{Mo}$  is the number of the Mo atoms in the hybrid system,  $E_{Mo}$  is the free energy of Mo atom (-10.592 eV),  $N_{S-2H}$  is the number of the S atoms in 2H domain part,  $E_{S-2H}$  is the energy of S atoms (-5.425 eV) in bulked 2H MoS<sub>2</sub> (subtract the energy of Mo atom from total energy of bulk system and divided by 2),  $N_{S-1T}$  is the number of the S atoms in 1T domain part,  $E_{S-1T}$  is the energy of S atoms (-5.128 eV) in bulked 1T MoS<sub>2</sub> (subtract the energy of Mo atom from total energy of bulk system and divided by 2), and  $d$  is the periodic length along the interface (0.55 nm for AC and 0.32 nm for ZZ).

As shown in Fig. 2, the formation energies of the hybrid systems for both AC and ZZ interface increase with the increase of the cell length. Increased formation energies indi-

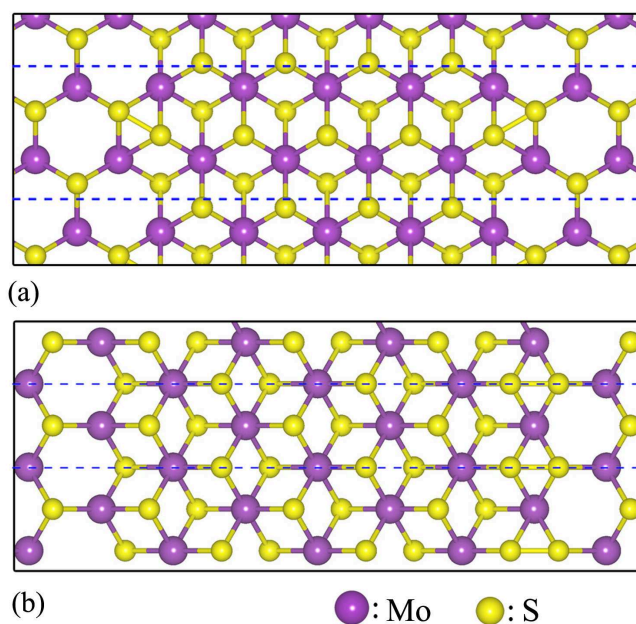


Figure 1: (Color online) Schematic models of single-layered MoS<sub>2</sub> heterostructures with (a) (armchair, AC) and (b) (zigzag, ZZ) interfaces. The blue dashed line labels the unit cell in (a) and (b).

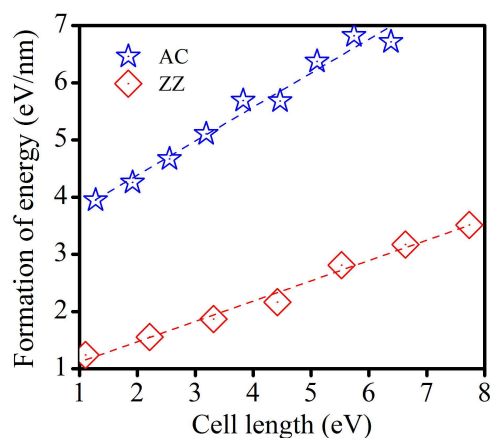


Figure 2: (color online) Formation energies of 1T/2H MoS<sub>2</sub> heterostructures with AC (blue stars) and ZZ (red rhombus) type interfaces as the function of cell length. The blue and red dashed lines are the linear fitting of the formation energies with the increase of cell length, AC:  $E_{form} = 5.78 + 1.075L$ , ZZ:  $E_{form} = 2.39 + 1.11L$ .

cated the broad interface effect, which make the atomic structures near the interface region can match perfectly with neither 2H nor 1T phase. For 1T/2H MoS<sub>2</sub> heterostructures with AC interface, 1T domains will deviate to 1T' structures [13]. And for 1T/2H MoS<sub>2</sub> heterostructures with ZZ interface, hybrid systems will be inflected with inflection angle 19.3 degree for the supercell length 4.422 nm and be wrinkled for larger supercell. This

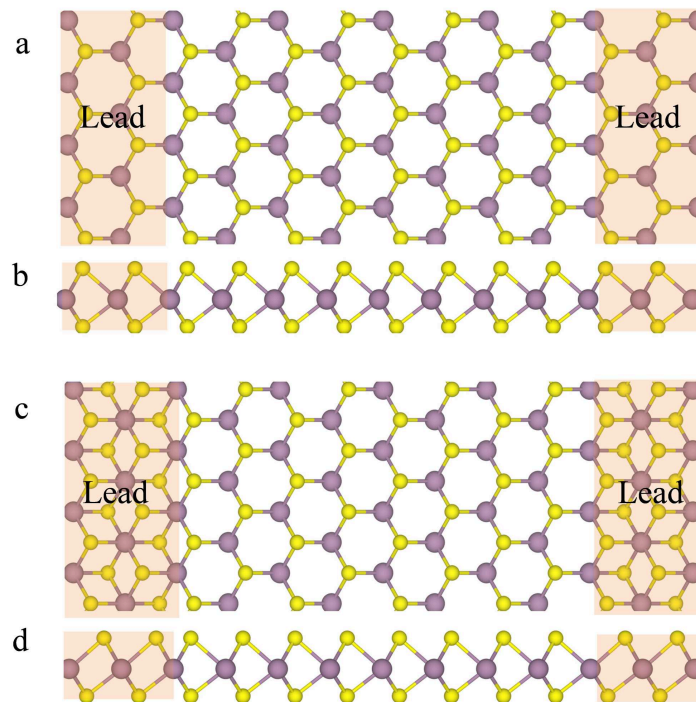


Figure 3: (Color online) Schematic models for two lead transport explorations on 2H MoS<sub>2</sub>. Top view (a) and side view (b) of the transport model with 2H MoS<sub>2</sub> itself as electrode (with shifted Fermi level for a metallic property). Top view (c) and side view (d) of the transport models with metallic 1T MoS<sub>2</sub> as electrodes and with ZZ interface.

kind of inflection and wrinkle has been reported in the polycrystalline graphene grain boundaries, which can relieve the mismatch strain and damage the ideal strength. [29] The variable behaviors (inflect or new T' phase) result from the interface effect make the formation energy different between AC and ZZ interfaces. From the linear fit as shown in Fig. 3, the formation energies of AC and ZZ interface can be extracted as 5.78 and 2.39 eV/nm. Then, 1T/2H MoS<sub>2</sub> heterostructure with ZZ interface is energies stable than that with AC interface. The present results are consistent with that in polycrystalline graphene and graphene/h-BN heterostructures, in which with ZZ type interfaces are more stable from the theoretical calculation and experimental observations [30–32].

## B. Transport properties

Transport explorations on the basis of fully relaxed structures of 2H MoS<sub>2</sub> have then been continued for with different electrodes as shown in Fig. 3. To take the 2H MoS<sub>2</sub> as the metallic electrode material, the Fermi level have been shifted to line up with the minimum of conductance band. In Fig. 3c and 3d, as a representatively example, devices with metallic 1T MoS<sub>2</sub> lead with ZZ interface is exhibited. Then, it is possible to explore the electrodes and interface effectes on the transports properties of 2H MoS<sub>2</sub>. The transport

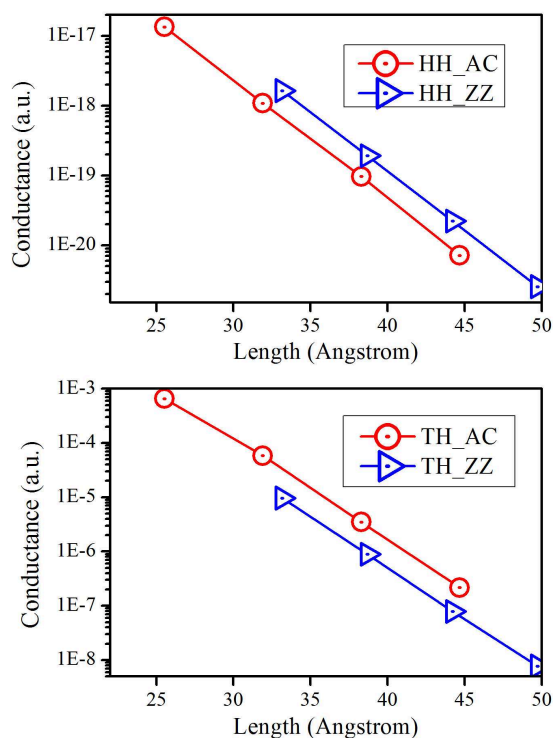


Figure 4: (Color online) The conductance of different width 2H MoS<sub>2</sub> with 2H (upper) and 1T (lower) electrodes along AC (red circle) and ZZ (blue triangle) interfaces.

properties under 2H and 1T electrodes can be found in Fig. 4. First of all, the conductance is reasonable decrease with the increase of transport width for both AC and ZZ directions with both 2H and 1T electrodes. Under the zero voltage, it should converge to zero with enough wide scattering regions. It can also be found that the conductance in AC and ZZ direction is relies on the electrode choice. For 2H electrode, conductance along the ZZ direction is slightly higher than that in AC direction. However, it is reversed for that with 1T electrode, conductance in AC direction is about ten times larger than that in ZZ direction.

In line with the experimental observations [16, 17], device with 1T electrode present much higher conductance compared to that with 2H electrode as shown in Fig. 4. One possible reason is that, even with shifted the Fermi level for 2H MoS<sub>2</sub> electrode, it's metallic performance is worse than 1T one because of lower carrier concentration. Another reason for the show up of the 1T/2H phase interface. Previous studies [24] also suggested that the tilt grain boundaries in polycrystalline MoS<sub>2</sub> can enhance its transport properties. The interface, result from the movement of S atoms, also can raise the conductance similar as grain boundaries.

To explore the deep relationship between the electrodes and the transport properties

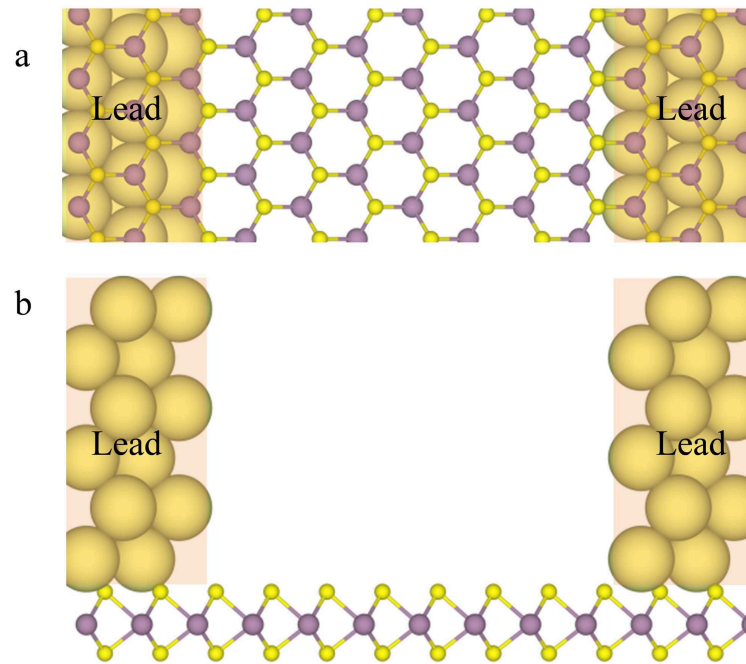


Figure 5: (Color online) Schematic models 2H MoS<sub>2</sub> with metal (Sc) electrodes from top side (upper) and side side (lower).

of 2D MoS<sub>2</sub>, device model with ZZ interface more close with the experimental measurement have been constructed as shown in Fig. 5. Bulk Scandium (Sc) have been deposited on and combined with 2H or 1T MoS<sub>2</sub> as electrodes. The introduce of metallic Sc make the transport direction changed from lateral transport limited in monolayer MoS<sub>2</sub> to vertical transport between bulk Sc and MoS<sub>2</sub>. In Fig. 6, the effects of metal Scandium can be found from the conductance difference for the scattering region width about 3 nm. Compared with that without metal Scandium, the conductance has been improved obviously for either 2H or 1T ones. However, the enhancements are quite different. For metallic Sc deposited on 2H electrodes, there is a profound effects compared with that with solo 2H electrodes, which suggested the carriers rarely from 2H MoS<sub>2</sub> and the low conductance in Fig. 4 is reasonable.

Moreover, the conductance is variable with the distance between the metal and 2H MoS<sub>2</sub>. The most stable configuration with about 1.85 angstrom distance corresponding the minor conductance. This conforms that the vertical transport direction between the bulk Sc and 2H MoS<sub>2</sub>. For case of metal Scandium deposited on 1T electrodes, the metal has moderate improvement compared with the former one. At the most stable point, the conductance is similar with that on 2H cases. In experimental measurement, the interface between metal and MoS<sub>2</sub> electrode is much complicated than the model in Fig. 5. Then, the metal enhancement will be more obvious and more sensitive. The above results indicated

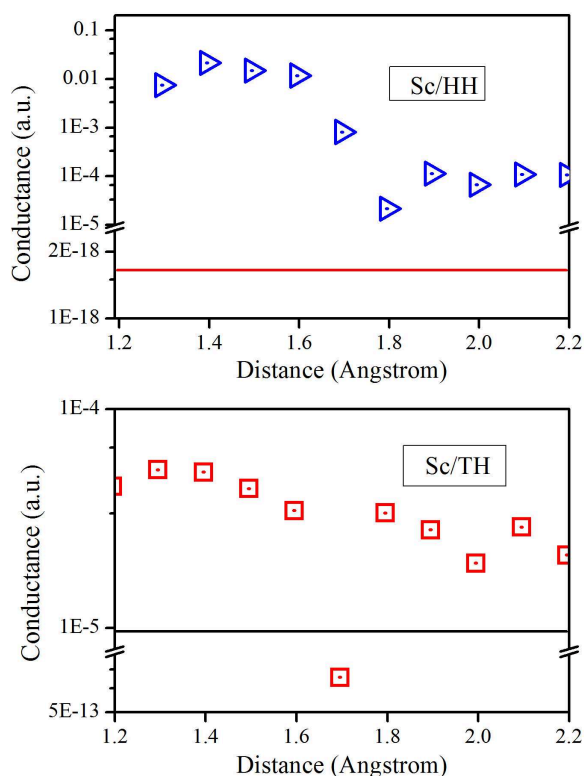


Figure 6: (Color online) The conductance 2H MoS<sub>2</sub> with Sc-2H MoS<sub>2</sub> (upper) and Sc-1T MoS<sub>2</sub> (lower) electrodes with different metal-MoS<sub>2</sub> distance.

that the transport properties of the device might depended not on the inject direction, but largely depended on the electrodes performance.

## 4 Conclusion

First-principles calculations have been carried out on the 1T/2H MoS<sub>2</sub> monolayer phase-heterostructures with AC and ZZ type interfaces. Hybrid system with ZZ interfaces are more energy favorable than AC by 3.39 eV/nm. Non-equilibrium calculation suggested the better transport properties by using the 1T phase MoS<sub>2</sub> from its higher conductance. The deposited metal on the electrodes can enlarge the conductance notably for MoS<sub>2</sub> with both 2H and 1T leads. Moreover, interface between 1T lead and 2H MoS<sub>2</sub> have large effect on the larger conductance compared with 2H leads. The present theoretical results can give the deep understanding for the experimental observations and future two dimensional electronic devices.

**Acknowledgments.** This work was supported by the Supported by Natural Science

Foundation of Shanxi province (No. 2015021011).

## References

- [1] K. F. Mak, C. Lee, J. Hone, J. Shan, and T. F. Heinz, *Phys. Rev. Lett.* 105, (2010) 136805.
- [2] B. Radisavljevic, A. Radenovic, J. Brivio, V. Giacometti, and A. Kis, *Nat. Nanotechnol.* 6,(2011) 147.
- [3] Z. Yin *et al.*, *ACS Nano* 6, (2011) 74.
- [4] K. F. Mak, K. He, J. Shan, and T. F. Heinz, *Nat. Nanotechnol.* 7, (2012) 494.
- [5] Q. H. Wang, K. Kalantar-Zadeh, A. Kis, J. N. Coleman, and M. S. Strano, *Nat. Nanotechnol.* 7, (2012) 699.
- [6] Y. Chen, J. Xi, D. O. Dumcenco, Z. Liu, K. Suenaga, D. Wang, Z. Shuai, Y.-S. Huang, and L. Xie, *ACS Nano* 7, (2013) 4610.
- [7] R. Ganatra and Q. Zhang, *ACS Nano* 8, (2014) 4074.
- [8] S. Bertolazzi, J. Brivio, and A. Kis, *ACS Nano* 5, (2011) 9703.
- [9] L. F. Mattheiss, *Phys. Rev. B* 8, (1973) 3719.
- [10] G. Eda, H. Yamaguchi, D. Voiry, T. Fujita, M. Chen, and M. Chhowalla, *Nano Lett.* 11, (2011) 5111.
- [11] B. Radisavljevic and A. Kis, *Nat. Mater.* 12, (2013) 815.
- [12] M. Kan, J. Y. Wang, X. W. Li, S. H. Zhang, Y. W. Li, Y. Kawazoe, Q. Sun, and P. Jena, *J. Phys. Chem. C* 118, (2014) 1515.
- [13] K.-A. N. Duerloo, Y. Li, and E. J. Reed, *Nat. Commun.* 5, (2014) 4214.
- [14] Y.-C. Lin, D. O. Dumcenco, Y.-S. Huang, and K. Suenaga, *Nat. Nanotechnol.* 9, (2014) 391.
- [15] G. Eda, T. Fujita, H. Yamaguchi, D. Voiry, M. Chen, and M. Chhowalla, *ACS Nano* 6, (2012) 7311.
- [16] R. Koppera, D. Voiry, S. E. Yalcin, B. Branch, G. Gupta, A. D. Mohite, and M. Chhowalla, *Nat. Mater.* 13, (2014) 1128.
- [17] R. Koppera *et al.*, *APL Materials* 2, (2014) 092516.
- [18] L. Ci *et al.*, *Nat. Mater.* 9, (2010) 430.
- [19] S. J. Haigh *et al.*, *Nat. Mater.* 11, (2012) 764.
- [20] Z. Liu *et al.*, *Nat. Nanotechnol.* 8, (2013) 119.
- [21] X. Duan *et al.*, *Nat. Nanotechnol.* 9, (2014) 1024.
- [22] G. Fiori, A. Betti, S. Bruzzone, and G. Iannaccone, *ACS Nano* 6, (2012) 2642.
- [23] M. P. Levendorf, C.-J. Kim, L. Brown, P. Y. Huang, R. W. Havener, D. A. Muller, and J. Park, *Nature* 488, (2012) 627.
- [24] S. Najmaei, M. Amani, M. L. Chin, Z. Liu, A. G. Birdwell, T. P. O'Regan, P. M. Ajayan, M. Dubey, and J. Lou, *ACS Nano* 8, (2014) 7930.
- [25] P. Blochl, *Phys. Rev. B* 50, (1994) 17953.
- [26] G. Kresse and D. Joubert, *Phys. Rev. B* 59, (1999) 1758.
- [27] J. P. Perdew, K. Burke, and M. Ernzerhof, *Phys. Rev. Lett.* 77, (1996) 3865.
- [28] K. S. Novoselov, D. Jiang, F. Schedin, T. J. Booth, V. V. Khotkevich, S. V. Morozov, and A. K. Geim, *Proc. Natl. Acad. Sci.* 102, (2005) 10451.
- [29] J. Zhang, J. Zhao, and J. Lu, *ACS Nano* 6, (2012) 2704.
- [30] J. Lahiri, Y. Lin, P. Bozkurt, I. I. Oleynik, and M. Batzill, *Nat nano* 5, (2010) 326.
- [31] J. Zhang and J. Zhao, *Carbon* 55, (2013) 151.
- [32] M. Liu *et al.*, *Nano Letters* 14, (2014) 6342.